A Thesis Entitled

Apoptosis and Cardiotoxicity Induced by Acute Methamphetamine Exposure in Larval Zebrafish (*Danio rerio*)

By

Hemaa Sree Kumar

Submitted to the Graduate Faculty as partial fulfillment of the requirements for the Master of Science Degree in Pharmacology and Toxicology

_____

Dr. Frederick Williams, Committee Chair

_____

Dr. F. Scott Hall, Committee Member

_____

Dr. Zahoor Shah, Committee Member

_____

Dr. Barry Scheuermann, Dean College of Graduate Studies

The University of Toledo

College of Pharmacy and Pharmaceutical Sciences

December 2020

An Abstract of

Apoptosis and Cardiotoxicity Induced by Acute Methamphetamine Exposure in Larval Zebrafish (*Danio rerio*)

By

Hemaa Sree Kumar

Submitted to the Graduate Faculty as partial fulfillment of the requirements for the Master of Science Degree in Pharmacology and Toxicology

The University of Toledo
December 2020

According to the 2020 World Drug Report, amphetamine type stimulant (ATS) is the third most used illicit drug with 27 million users globally. Methamphetamine (MA) is a potent central nervous system (CNS) stimulant with a high abuse potential and addiction. MA use has become an increasing concern worldwide especially due to the adverse effects it possesses. MA is also known as the poor man's cocaine since it is more easily accessible "illegally" and inexpensive compared to cocaine. The euphoric feeling from MA also lasts longer than cocaine due to its long half-life (10-12h) and lipophilicity that allows MA to better penetrate the blood brain barrier (BBB) easily. The primary aim of this study was to study the acute toxic effects of MA that may contribute to acute lethality as well as to long-term adverse effects associated with MA use. The hypothesis of this study is that death in 5-dpf larval zebrafish is due to apoptosis in the cardiovascular system and/or in the brain secondary to acute MA exposure.

MA works by causing an increase in the levels of dopamine (DA), norepinephrine (NE), serotonin (5-HT) and preventing the re-uptake of these neurotransmitters (NT) by

blocking monoamine transporters, which then increases the levels of the NT in the synaptic cleft. An increase in DA, NE, 5-HT causes users to experience intense euphoric feelings, increased heart rate (tachycardia), hyperthermia, increased energy, hypertension and decrease in appetite. Some of the chronic abuse of MA leads to neurotoxicity, agitation, aggression, anxiety, psychosis, renal and liver failure, seizure, and cardiac arrhythmias, heart attacks. In this study, we used 5-day old larval zebrafish and exposed them to three different concentrations (0mM, 5mM and 15mM) of MA for 5-hr to assess change in heart rate and other lethality parameters such as lack of heartbeat, opaque appearance and notochord bend (lordosis). Subjects were then processed for cleaved caspase-3 immunofluorescence assay and Western Blotting. Change in heart rate for subjects in 5mM group was not significant. Conversely, significant decline in heart rate was observed in the 15mM cohort as the duration of exposure increases starting at 1h time point. Cell death which could be due to the apoptosis involving caspase-3 involving otolith, hindbrain, notochord and caudal tail was observed via immunofluorescence staining. Apoptosis was found to be more significant in the 15mM cohort. There seem to be an involvement of the cardiovascular (CV) system secondary to acute MA exposure, however, the mechanisms involved in cell death is unclear. Additional studies and different techniques could be utilized in future studies to elucidate a mechanism that may be contributing to cell death following acute exposure to MA.

Acknowledgements

I would like to express my sincere gratitude to my advisor, Dr. Frederick Williams for his continuous support, patience and advice. I would also like to thank my committee members Dr. F. Scott Hall and Dr. Zahoor Shah for being a tremendous help and providing valuable comments. I also would not have been able to execute some of the essential tasks required without the courtesy of Dr. Zahoor Shah and everyone in his laboratory for allowing me to work within his laboratory. A special thanks to Daniyah Almarghalani and Hannah Saternos for assisting me with the Western Blot techniques and data analysis.

I would like to express my deepest appreciation to Dr. Alexander Wisner for providing invaluable guidance, insightful comments and encouragement throughout my research project. I would also like to thank my lab mates; Jillian Dietrich, Kabita Gwachha, Sasha Heeren, Sidney Ley and Yu Chen for their generous attitude and constructive advice. Thank you for making graduate school a little less stressful.

I would like to thank my family for their unwavering support and love even from miles away. I'd also like to extend my gratitude to my friends. Thank you for listening, for your words of encouragement and supporting me through this entire process.

Lastly, I also wish to thank Dr. Caren Steinmiller, Dr. Holiday-Goodman, and Dr. Kimberly Jenkins for always being there with a word of encouragement, Holly Helminski and everyone in the College of Pharmacy and Pharmaceutical Sciences at the University of Toledo for being accommodating. It has been an interesting journey for me but has helped me gain valuable experience and lifelong connections, and for that I will always be grateful.

Table of Contents

List of Tables

List of Figures

Chapter 1

Introduction

1.1 Zebrafish

1.1.1 Zebrafish as Model Species

Zebrafish, (*Danio rerio)* is a tropical freshwater vertebrate that is native to South Asia. They are broadly distributed across parts of India, Bangladesh, Nepal, Pakistan and Myanmar (Lawrence 2007) and are typically found in slow moving water bodies such as lakes, rivers and ponds. They also prefer shallow, moderately clear water as well as warm water temperatures (~28°C). Zebrafish get their names due to the appearance of the alternating blue-black stripes on the side of the body (Reed and Jennings 2011). The onset of pigmentation usually starts at ~48-hours post-fertilization and is more prominent in their adult stages (2-3 months old) (Reed and Jennings 2011) as shown in Figure 1 and 2.

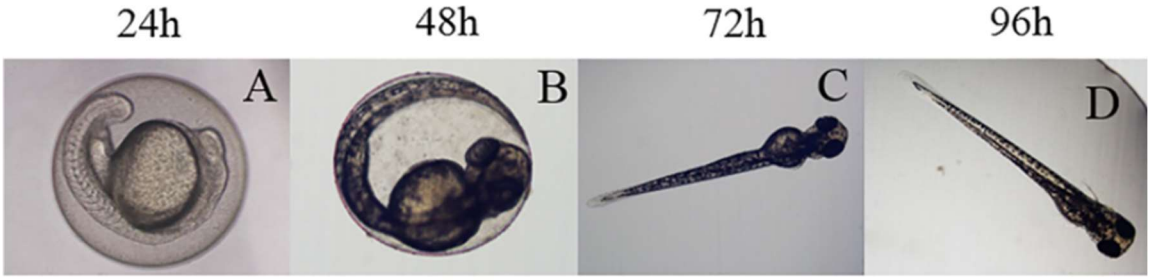

Figure 1. Zebrafish (AB strain) developmental stage at 24h (A), 48h (B), 72h (C) and 96h (D) post fertilization showing normal appearance with onset of pigmentation starting in (B). Source of image: (Mao, Jia et al. 2020).

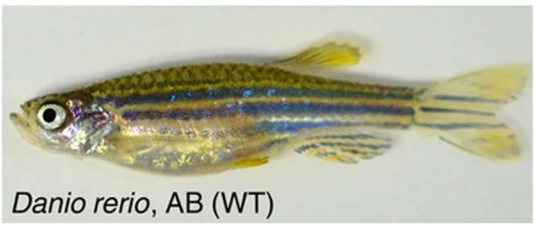

Figure 2. Adult zebrafish (AB strain) showing more prominent pigmentation. (Antinucci and Hindges 2016)

The use of zebrafish in research began in the 1960s and has been increasing progressively as a model organism (Reed and Jennings 2011). Zebrafish is used to investigate developmental mechanisms in vertebrates, as well as questions in genome evolution, molecular biology, developmental biology, genetic research, physiology and toxicology (McCluskey and Postlethwait 2015). Recently, they have also been used in cancer research, drug discovery and for photoaffinity labeling to investigate protein targets of drugs. A mutant zebrafish strain, termed "Casper" zebrafish was used in *in vivo* photoaffinity labeling study as this strain allows *in vivo* fluorescent analysis due to their transparent appearance as adults (Tackie-Yarboi, Wisner et al. 2020).The specialized and definitive assets of the zebrafish model make it a crucial model species (Gut, Reischauer et al. 2017). One of the advantages of using zebrafish as an animal model instead of other animal models such as rodents, (e.g. mice) is cost efficiency, especially when it comes to maintaining a colony. Zebrafish are a shoaling species and highly social so they can be housed together with other fish at a high density (Reed and Jennings 2011). Adult zebrafish are also fairly small in size (2.4 – 4cm) which means they take up less space and are inexpensive to sustain (Burke August 9, 2016). Their small size also allows for phenotypic screening in multi-well plates. Furthermore, zebrafish also have a high fertilization rate as they can breed all year. Adult female zebrafish can produce eggs every week between 70

to 300 eggs, of which at least 80% are fertilized (Reed and Jennings 2011). Zebrafish eggs are fertilized and developed outside the mother's body permitting the use of the organism at early developmental stages as well as for *in vitro* (drug and toxicity) studies if necessary. They also have significant potential for high-throughput screening (Kalueff, Gebhardt et al. 2013) because of their rapidly developing vertebrate body plan where they lay clear eggs that develop into translucent embryos within ~24 hours post-fertilization (hpf). The transparent characteristics of larval zebrafish allow researchers to look for any kind of normal/abnormal development, organs, biological processes, and other parameters (e.g.: heart rate) under a microscope without using any invasive techniques. At approximately 3-6 months old, most of them are sexually mature and can be used for breeding in a laboratory setting. This can differ as it is reliant on the management of zebrafish husbandry (Lawrence 2011). All their major organ systems, including a beating heart, major vessels with circulating blood, and a rudimentary gut are fully formed by 48 hpf (Gut, Reischauer et al. 2017). Moreover, as a vertebrate, they have similar major organs and tissues as humans. Zebrafish also share approximately 70% of homology with the human genome and 82% of orthologous human disease-related genes (Gutierrez-Lovera, Vazquez-Rios et al. 2017).

1.1.2 Zebrafish Cardiovascular System

The heart is one of the first organs to be formed during organogenesis in the early developmental stage in zebrafish (Stainier 2001). Zebrafish heart is a single closed circulatory system that is comprised of two chambers with four components: sinus venous, atrium, ventricle and bulbous arteriosus as shown in Figure 3 (Gut, Reischauer et al. 2017, Galanternik, Stratman et al. 2020). It should be noted that zebrafish embryos can use passive diffusion to receive oxygen to survive in the event of a dysfunctional cardiovascular system for several days due to their comparatively small size. This allows an opportunity for studying gene function and a thorough analysis to be done in animals with heart defects (Stainier 2001, Bakkers 2011). Although there might be some difference between the mammalian and zebrafish heart, zebrafish do have substantial anatomic and physiological similarities that can be of an advantage for cardiovascular related research. One of them is that the zebrafish heart matures from a linear heart tube that develops (~24hpf) when the mesodermal progenitors' fuse together and it begins beating via peristaltic motion (Gut, Reischauer et al. 2017). Also, the zebrafish heart beats at 120-180 beats per minute (bpm), which is close to the heart rate of human (60-100 bpm) (Poon and Brand 2013). The atrial and ventral chambers are separated by valves to ensure blood flow in the right direction as shown in Figure 3. The zebrafish heart is also designed to pump oxygenated blood throughout its body. Blood enters the heart via sinus venous and passes through the atrium and ventricle. The atrium acts as a collecting chamber of the heart. The ventricle then pumps the deoxygenated blood from the atrium into the bulbous arteriosus to the ventral aorta to distribute to the gills for oxygenation of the blood (Asnani and Peterson 2014, Galanternik, Stratman et al. 2020)

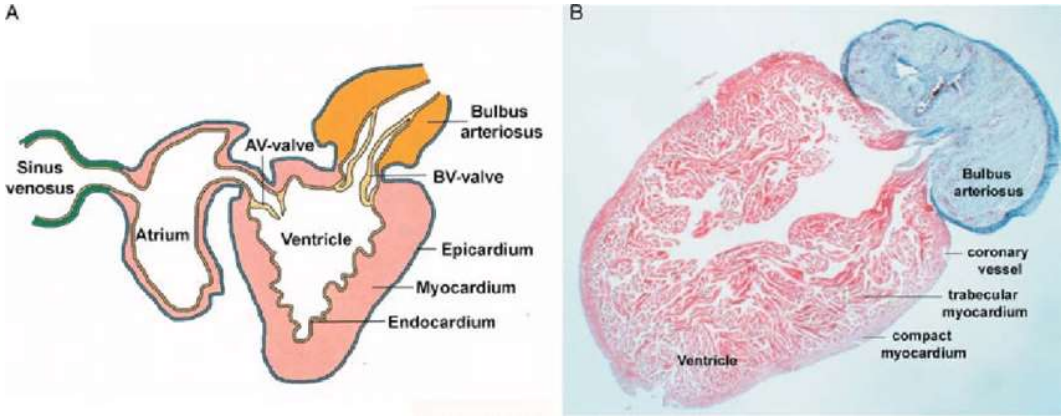

Figure 3. Anatomy of the adult zebrafish heart. (A) Graphic representation of the heart of an adult zebrafish. AV stands for atrioventricular valve and BV stands for bulboventricular valve. (B) Trichrome stained histological section the ventricle and bulbous arteriosus (Poon and Brand 2013).

1.1.3 Zebrafish Central Nervous System

Zebrafish brain development occurs within 3 days post-fertilization, together with the central nervous system (CNS)(d'Amora and Giordani 2018). By 24hpf, the forebrain (most anterior), midbrain and hindbrain (most posterior) can be broadly defined and easily distinguished (Figure 4)(Vaz, Hofmeister et al. 2019). Zebrafish possess a high degree of genetic, morphological and physiological homology with humans (d'Amora and Giordani 2018). Zebrafish nervous system's main architecture resembles that of the mammals, despite differences in the development of the telencephalon and mesodiencephalon (Panula, Chen et al. 2010). For instance, zebrafish's medial teleost pallium has homologous structures to mammalian amygdala (Portavella, Torres et al. 2004, Mueller, Dong et al. 2011, von Trotha, Vernier et al. 2014) which is a key structure for affective processing and emotions in humans (Khan, Collier et al. 2017). Although the number of G protein-coupled receptors in zebrafish is larger (due to gene duplication) than in mammals (Panula, Chen et al. 2010), many receptors have similar expression patterns, binding and signaling

properties as in mammals. Distinct differences between mammals and zebrafish include duplication of the tyrosine hydroxylase (TH) gene in zebrafish, and presence of one instead of two monoamine oxidase (MOA) genes (Panula, Chen et al. 2010). Detection of 3-methoxytyramine (3-MT) in whole fish at 5 dpf means that the enzymes responsible for their production are active in larval zebrafish (Sallinen, Sundvik et al. 2009). Based on expression patterns, it can be expected that TH1 may be responsible for production of L-DOPA and dopamine in the noradrenergic pathway (Panula, Chen et al. 2010). Neurochemistry is generally conserved across vertebrates as they share majority of the neurotransmitters, receptors and transporters (Khan, Collier et al. 2017). Zebrafish are found to be sensitive to major classes of drugs such as psychostimulants, opiates, hallucinogens, ethanol, anxiolytics, antidepressants and antipsychotics (Khan, Collier et al. 2017).

Development of the blood-brain barrier (BBB) in zebrafish has recently been characterized by (Jeong, Kwon et al. 2008), showed that it shares similar properties with young mouse embryos when zebrafish are in their early developmental stage (3-5 dpf) (Panula, Chen et al. 2010). Expression of tight junction molecules Claudin-5 and Zonula Occludens-1 (ZO-1) in cerebellar endothelial cell junctions suggest that BBB of zebrafish is functionally and molecularly similar to that of higher vertebrates (Jeong, Kwon et al. 2008).

Although all these features above make zebrafish an attractive animal model to study neurotoxicity, some limitation may include not being able to control the chemical dose absorbed since zebrafish embryos are not developing inside a placenta and are exposed to chemicals in medium and absorb them directly (Rubinstein 2006). In addition,

chemicals can be metabolized differently than in mammals (d'Amora and Giordani 2018). (Panula, Chen et al. 2010) suggest that metabolism of DA and NE can be dependent on catechol-O-methyltransferase (COMT). COMT is not well characterized but detection of 3-methoyxtyramine (3-MT) suggests a presence of COMT (Panula, Chen et al. 2010).

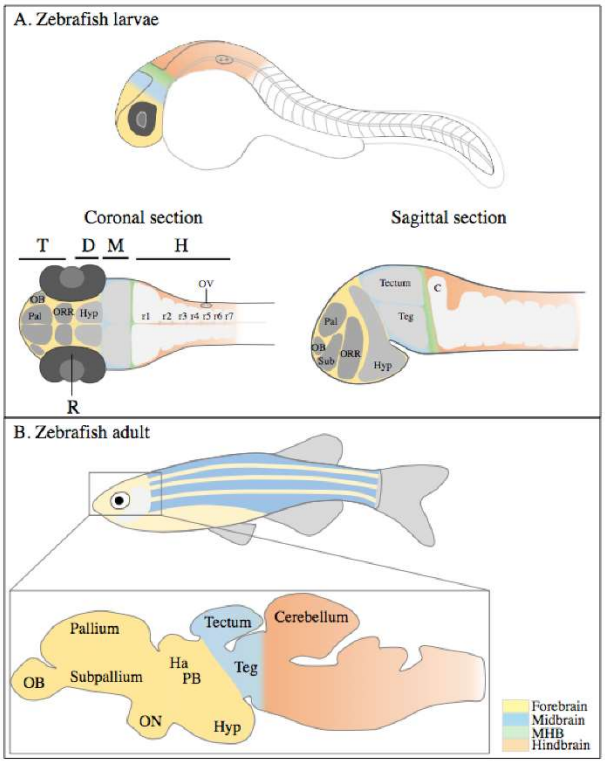

Figure 4. (A) Representative image of the embryonic brain at 30 hpf, showing the forebrain (in yellow), midbrain (in blue), MHB (in green), and hindbrain (in orange). Coronal and sagittal section schemes show brain structures primordia. Forebrain is subdivided in the telencephalon (in darker gray) and the diencephalon (containing the hypothalamus, lighter grey). (B) Simplified representation of the adult brain and main domains. Drawings not to scale; C: cerebellum; D: diencephalon; M: midbrain; MHB: midbrain-hindbrain boundary; H: hindbrain; Ha: habenula; Hyp: hypothalamus; OB: olfactory bulb; ON: optic nerve; ORR: optic recess region; OV: otic vesicle; Pal: pallium; PB: pineal body; R: retina; r1–r7: rhombomeres 1 to 7; Sub: sub-pallium; T: telencephalon; and Teg: tegmentum. Image adapted from (Rink and Wullimann 2002, Vaz, Hofmeister et al. 2019)

1.2 Methamphetamine Hydrochloride

1.2.1 History of Methamphetamine

Methamphetamine (MA; *N*-methyl-*O*-phenyliso-propylamine) is a derivative of amphetamine and a psychostimulant that activates the CNS and the sympathetic nervous system (Anglin, Burke et al. 2000, Kevil, Goeders et al. 2019). Due to its sympathomimetic effect there is an increase in heart rate, blood pressure and decrease in appetite that is experienced. Some other acute effects that MA user experience are feelings of euphoria, increased energy and increased libido. According to the World Drug Report 2020 by the United Nations Office on Drugs and Crime (UNODC), MA use has been on the rise in North America since 2018. In the United States specifically, 0.7 per cent of the population which translates to 1.9 million people aged 12 and older has reported the use of MA in the past year (Drugs and Crime 2020). Rate of death due to drug overdose involving psychostimulants (amphetamines, MA and methylphenidate) increased nearly five-fold (from 0.8 to 3.9) which accounts for an increase in 30% on average per year from 2012 through 2018 (Hedegaard, Miniño et al. 2020). MA also produces serious adverse effects on many organ systems, mainly the central nervous and the cardiovascular system (Sun, Wang et al. 2019). MA can be smoked, ingested orally, snorted, injected or dissolved sublingually (Courtney and Ray 2014). The effect of the intense “rush” or “high” is more common when MA is smoked and is almost instantaneous when injected (Anglin, Burke et al. 2000). Crystal meth (crystalline solid form of MA) is one of the more prevalent smokable forms (Kish 2008). MA is a Schedule II drug under the Controlled Substances Act with a very high abuse potential and is typically used as a recreational drug . Meth,

Speed, Ice, Crystal, Shards, Bikers Coffee, Crank, Shabu are some of the street names for MA (NIDA 2019).

MA was first synthesized from ephedrine in 1893 by a Japanese pharmacologist. MA gained popularity when it was widely used by military personnel during the World War II to increase their performance and stamina (Anglin, Burke et al. 2000). MA's first medical use was to treat asthma due to its bronchial dilation properties (Anglin, Burke et al. 2000). Today, Desoxyn® is the only drug containing methamphetamine hydrochloride that is approved by the FDA and can be legally prescribed in the United States. Desoxyn® is indicated for short-term treatment of obesity and attention deficit with hyperactive disorder (ADHD) (Kish 2008). The highly addictive nature of MA could explain the unpleasant withdrawal symptoms MA users' experience. Some of the withdrawal symptoms (partly due to low levels of dopamine) are extreme depression, aggression, lethargy, cognitive impairment, anergia, irritability and intense MA craving (Anglin, Burke et al. 2000, Courtney and Ray 2014).

1.2.2 Mechanism of Action of Methamphetamine

MA is an indirect agonist at dopamine (DA), norepinephrine (NE) and serotonin (5-HT) receptors. It works by causing an increase in the levels of these neurotransmitters in the synaptic cleft (Cruickshank and Dyer 2009, M Chiu and O Schenk 2012). MA is also highly lipophilic due to the addition of methyl group in its structure allowing it to cross the blood brain barrier easily and enter the brain quickly (Kevil, Goeders et al. 2019). MA works by activating reward and reinforcement systems in the brain, including the mesolimbic dopamine pathway in the brain (M Chiu and O Schenk 2012). The reward pathway is responsible for controlling behavior and memory. It provides positive

reinforcement when activated by natural rewards like food, water and sex or via drug rewards like cocaine, alcohol, nicotine and amphetamines (M Chiu and O Schenk 2012). The mesolimbic pathway consists of the ventral tegmental area (VTA) which connects to the nucleus accumbens (NAc) and the prefrontal cortex (PFC), median forebrain bundle and the limbic system (M Chiu and O Schenk 2012, Merritt 2019). When neurons that contain dopamine (DA) in the VTA are activated dopamine released in the NAc and the prefrontal cortex in response to novel and highly salient stimuli (AOAAM 2019), or stimuli that have come to be associated with those stimuli. Under normal conditions, when the reward pathway in the brain is activated, dopamine from synaptic vesicles is discharged into the synapse, and binds to post-synaptic receptors. Extra-synaptic dopamine is taken up by the dopamine-transporter (DAT) and translocating back into the presynaptic element (M Chiu and O Schenk 2012). (Yifan Xiao , M Chiu and O Schenk 2012, Ickes 2015, 2016, NIDA 2016). NE and 5-HT have analogous release and uptake mechanisms with specific membrane transporters, but the same vesicular transporter, VMAT2 (M Chiu and O Schenk 2012). MA works partly by preventing the re-uptake of DA, NE and 5-HT into the pre-synaptic space by inhibiting their respective transporters; dopamine transporter (DAT), norepinephrine transporter (NET), serotonin transporter (SERT) owing to the structural similarity that MA share with these neurotransmitters (M Chiu and O Schenk 2012, Courtney and Ray 2014, Kevil, Goeders et al. 2019). This leads to an increased concentration of DA, NE and 5-HT in the synapse and overstimulation of the postsynaptic monoamine receptors (Kevil, Goeders et al. 2019). However, unlike drugs that act solely as reuptake inhibitors, MA is also a transporter substrate, passing into the cell where MA also reverses the function of VMAT-2 protein causing its vesicular contents to be released

into the cytosol and causing reverse transport via the membrane transporters, which further amplifies extra-synaptic levels of these neurotransmitters (Cruickshank and Dyer 2009). Increased levels of DA in the cytosol characteristic of releasing agents such as MA contributes to formation of reactive oxygen species (ROS) by auto-oxidation (Cruickshank and Dyer 2009, Sofuoglu and Sewell 2009, M Chiu and O Schenk 2012). MA's long half-life (~12 hours in humans) contributes to excess DA lingering in the synapse for an extended period, while the initial surge in dopamine levels contributes to euphoria and the initial conditioned responses at early stages of the addictive process (M Chiu and O Schenk 2012, 2016, NIDA 2016, Kevil, Goeders et al. 2019). Counter adaptations associated with chronic MA administration are associated with withdrawal symptoms and later stages of MA addiction, dependence, and long-term adverse effects (Koob 1992, Cadet, Jayanthi et al. 2005).

In the case of norepinephrine (NE), it is derived from DA, with NE neurons containing an extra enzyme, dopamine-β-hydroxylase that converts DA to NE. Due to MA's effect blocking NET preventing re-uptake, and producing reverse transport via NET, there will be an increase in levels of NE in NE terminal regions including the hippocampus, PFC, and medial basal forebrain (Cruickshank and Dyer 2009, Courtney and Ray 2014). Increased NE levels are associated with increased arousal and wakefulness, mydriasis, alertness, elevated heart rate, blood pressure, body temperature and various cognitive effects

Serotonin (5-HT) is a monoamine neurotransmitter that is synthesized in the pre-synaptic vesicle and its receptors are found all throughout the brain region regulating functions like sex drive, higher cognitive processing, respiration, pain perception, satiety,

and anxiety (M Chiu and O Schenk 2012, Courtney and Ray 2014). Effects of MA on 5-HT is similar to those on DA. MA inhibits the re-uptake of 5-HT by blocking its transporter (SERT), causing a rise in the levels of 5-HT in the synaptic cleft similar to the action of DA (M Chiu and O Schenk 2012). A single dose of MA (15mg/kg) causes a decrease in tryptophan hydroxylase (rate limiting enzyme in 5-HT synthesis) in the NAc and caudate based on a review by (Haile 2008). It is also worth noting that MA binds to SERT at a much lower affinity compared to DAT and NET (Rothman, Baumann et al. 2001). In particular, MA binds to NET at a much higher affinity compared to DAT releasing NE more potently than DA and much more than 5-HT (Ferrucci, Limanaqi et al. 2019).

Last but not least, MA also impairs the metabolism of the monoamine oxidase (MAO). MAO-A/-B iso-enzymes are responsible in deaminating DA, NE, and 5-HT. MAO-A (placed within synaptic terminals of DA and NE neurons) is competitively inhibited by MA at a higher affinity than MAO-B (placed within 5-HT terminals and non-catecholamine neurons) (Ferrucci, Limanaqi et al. 2019). Decrease in the activity of MAO causes a rise in the levels of these monoamines (Cruickshank and Dyer 2009, Courtney and Ray 2014). This last action, in combination with the others, is critical for the neurotoxic effects of amphetamine-like stimulant drugs such as MA. Attenuation of presynaptic storage of monoamines as well as downregulations of receptors is evidenced at high doses or with chronic use of MA (Courtney and Ray 2014). Additionally, it also causes formation of reactive oxidative species (ROS) which contributes to MA-associated neurotoxicity and cardiomyopathy (Sofuoglu and Sewell 2009, M Chiu and O Schenk 2012, Courtney and Ray 2014, Reddy, Ng et al. 2020). Chronic MA use can also cause “meth mouth”, visual and auditory hallucinations, paranoia, hyperthermia, formation of abscess at site of

injection, cerebral hypoperfusion and cardiovascular effects like stroke, cardiac arrhythmia or sudden cardiac death (Anglin, Burke et al. 2000, Cruickshank and Dyer 2009, M Chiu and O Schenk 2012, Kevil, Goeders et al. 2019).

To translate the mechanism of action of MA in zebrafish, it is shown that zebrafish demonstrates sensitivity to MA (Khan, Collier et al. 2017). Based on the review by (Khan, Collier et al. 2017), it is shown that acute MA administration induces avoidant behavior, increase in swimming speed and mirror stimulation task.

1.2.3 Effects of Methamphetamine on the Cardiovascular System

It is no surprise that MA use exerts an influence on the cardiovascular system. A major emphasis of studies into the chronic effects of MA have focused on neurotoxic effects. However, cardiovascular complications in MA users are thought to be the second leading cause of death (Paratz, Cunningham et al. 2016), yet the mechanisms involved in cardiotoxicity are much less understood. According to (Sun, Wang et al. 2019), a study of 100 human deaths by (Akhgari, Mobaraki et al. 2017), showed that at least 68% of the cases had pathological cardiovascular abnormalities such as cardiomyocyte hypertrophy, focal degeneration, necrosis and atherosclerosis. The high levels of catecholamine (specifically DA and NE) released from sympathetic nerve endings due to MA's mechanism of action is thought to result in adverse cardiovascular effects like vasoconstriction, vasospasm, tachycardia, hypertension and increased myocardial contractility (Kaye, McKetin et al. 2007, Kish 2008, Kevil, Goeders et al. 2019). Additionally, those symptoms are also commonly seen in patients that were admitted due to MA overdose (Kaye, McKetin et al. 2007). Acute coronary syndrome, acute myocardial infarction, aortic dissection and sudden cardiac death are some of the infrequent

cardiovascular events seen with acute MA use (Kaye, McKetin et al. 2007). Chronic MA users are at a higher risk for coronary artery diseases (e.g. pulmonary hypertension) due to vasoconstriction in smooth muscle and reduced sensitivity to nitric oxide (Kevil, Goeders et al. 2019), cardiomegaly (enlarged heart), cardiomyopathy (Kaye, McKetin et al. 2007) and possibly modulation of reactive oxygen species (ROS) (Reddy, Ng et al. 2020). MA associated cardiomyopathy, which is commonly seen in MA users, is thought to be caused due to direct and indirect myocardial damage. Direct myocardial damage can occur due to multiple pathways: augmented free radical production promoting ROS, apoptosis due to increased p-53 activity, decreased function of mitochondria, altered gene expression and defects in the intracellular calcium homeostasis (Reddy, Ng et al. 2020). Several studies also show that MA use can induce apoptosis in cardiomyocytes (Leung, Qu et al. 2014, Sun, Wang et al. 2019) although the exact mechanism is still ambiguous. (Reddy, Ng et al. 2020) suggested that apoptosis might be due to an increase in the activity of p-53 which can cause direct myocardial damage in the event of MA associated cardiomyopathy. p-53 is a tumor suppressor protein that plays a vital role in prevention of cancer by removing excess, injured or septic cells through apoptosis (Haupt, Berger et al. 2003). p-53 is stimulated when there is a presence of external or internal stress which then encourages apoptosis and inhibits cell growth for cells that are hypoxic or with damaged DNA (Haupt, Berger et al. 2003).

1.3 Role of Caspase in Apoptosis

Apoptosis is a highly regulated programmed cell death and a vital component of health and disease. Dysfunctions of apoptosis or excess apoptosis can contribute to many disease states. Apoptosis helps eradicate cells during development and pre-cancerous cells or cells with damaged DNA, as well as playing a key role in maintaining a healthy immune system. Apoptosis can occur via two signaling pathways, extrinsic and intrinsic. The extrinsic pathway involves binding of ligands to cell surfaces on death receptors whereas the intrinsic pathway involves the mitochondria and is activated when there is DNA damage due to oxidative stress or as a result of other intracellular signals (Hooper and Killick , Elmore 2007). Both the extrinsic and intrinsic pathways induce cell death via caspase-mediated apoptosis (Moorjani, Ahmad et al. 2006). Caspases are aspartate-specific cysteine proteases that break down proteins into smaller fragments. Once a caspase cascade is initiated, it is thought to cause an irreversible cell death. There are 10 major caspases that have been identified and are broadly categorized into three different categories: initiator caspases, effector caspases, inflammatory caspases and others. Initiator caspases include caspase-2, caspase-8, caspase-9, and caspase-10; effector caspase include caspase-3, caspase-6, and caspase-7; inflammatory caspase include caspase-1, caspase-4, and caspase-5; while other caspases include caspase-11, caspase-12 and caspase-14 (highly expressed in embryonic tissue but not in adults) (Hooper and Killick , Elmore 2007). Caspases -3, -8 and -9 are also thought to be crucial in apoptosis involving cardiomyocytes (Moorjani, Ahmad et al. 2006). Activation of caspases -8, -9, and -10 can initiate the activation of the execution pathway via activity of caspase-3 which eventually leads to formation of apoptotic bodies (Moorjani, Ahmad et al. 2006). The diagram used by Elmore

(2007) as shown in Figure 5 outlines a brief summary of the pathways involved in caspase activation for apoptosis to occur.

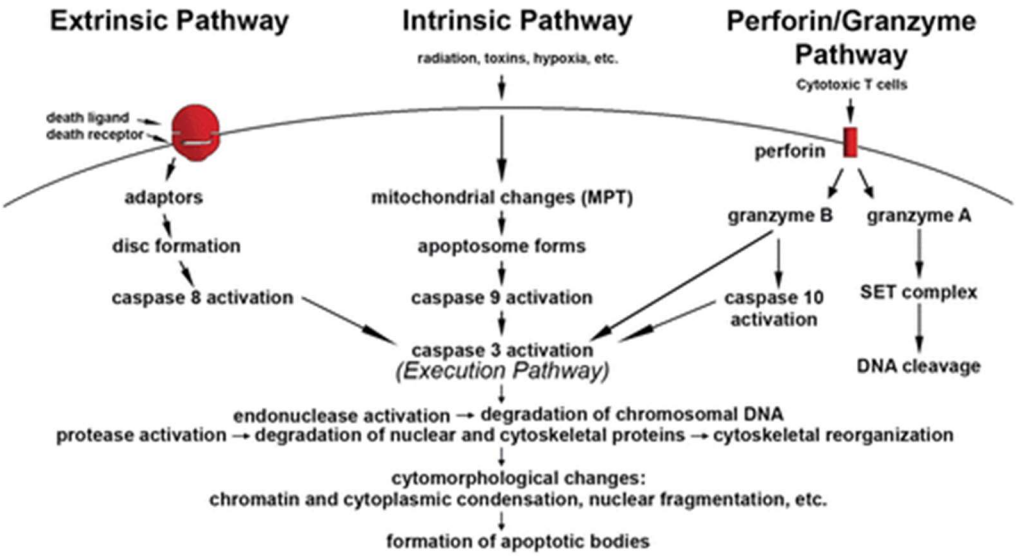

Figure 5. Illustrative diagram of pathways involved in apoptosis. Each pathway requires their own signal which triggers the activation of initiator caspase for their respective pathway which then leads to activation of the execution cascade by caspase-3 activation (Elmore 2007).

1.4 Objective and Hypothesis

The objective of this study was to assess the acute toxic effects of MA that may contribute to acute lethality as well as to long-term adverse effects associated with MA use. The hypothesis for this study is that death in 5-dpf larval zebrafish is due to apoptosis in the cardiovascular system and/or in the brain secondary to acute MA exposure.

Chapter 2

Materials and Methods

2.1 Zebrafish Husbandry

AB strain (wild type) adult zebrafish were obtained from an in-stock population in the Zebrafish CD3 Lab (HEB 013 G/H) at the University of Toledo (Toledo, OH, USA) for breeding. The original source of zebrafish used to maintain in-stock colony is from Zebrafish International Resource Center (ZIRC). The adult zebrafish were raised at ~27-29 ˚C on a 14:10 h light-dark cycle. There are approximately 8-10 adult zebrafish in each full-sized tank filled with system water and are separated by sex. They are fed once daily with live brine shrimp (*Artemia salina*) on Monday, Wednesday and Friday and flake food the rest of the days. Male and female adult zebrafish were placed together in a breeding tank (1:2 ratio) and left overnight in the Zebrafish CD3 Lab. Embryos were collected and cleaned (removing any unfertilized embryos or fecal material) the next morning. Once they are cleaned, embryos are stored in a petri dish with egg water in the incubator at ~28˚C. Eggs are then cleaned, and any unfertilized embryos or chorions were removed at least once a day up until 5 days post fertilization (dpf). Any excess larval zebrafish that were not used in the experiments were euthanized in an ice bath following standard procedures. All procedures were carried out in compliance with the Institutional Animal Care and Use Committee at the University of Toledo (IACUC) (Protocol number: 105414).

2.2 Materials

2.2.1 Drug Treatment and Immunofluorescence Staining

MA was obtained from Sigma-Aldrich (St. Louis, Mo.) under the supervision of Dr. F. Scott Hall, Associate Professor in the Department of Pharmacology and Experimental Therapeutics, University of Toledo, Toledo, OH, USA (Lot no: SLBV9808, Sigma Aldrich). 112 mg of MA was dissolved in 6 ml of egg water (DI water with pH of 7.6 and adjusted salinity, autoclaved at 121 ºC) to make a stock solution of 100 mM which was then aliquoted into five-100 mM stock solution, stored in -80 °C. Egg water was used as a vehicle for control. All guidelines applying to handling Schedule II drugs/substances were followed. Antibodies were purchased from Abcam Inc. Primary Antibody used was Anti-Caspase-3 Antibody (Lot no: ab13847). Secondary Antibody used was Donkey Anti-Rabbit IgG H&L (Alexa Fluor®488) (Lot no: ab150073). Cell culture reagents were obtained from the following sources: 1X PBS, 1x PBST, Acetone (Lot no: 116111, Fischer Scientific), 10% Formalin, DMSO (Lot no: 20684, Pierce™, IL, USA), Methyl-cellulose (Lot no: 795356, Fischer Scientific Company), Fetal Bovine Serum, Albumin, Bovine BSA Heat Shock (Lot no: 30227-40149, Research Product International, IL, USA), Triton-X 100 (Lot no: 036262, Fischer Biotech), Tween-20 (Cat no: 1706531, Bio-Rad). Eppendorf tubes were used to collect larval zebrafish after fixation.

2.2.2 Homogenization of Larvae and Protein Quantification

Materials used to homogenize subjects were radioimmunoprecipitation assay (RIPA) buffer [sodium fluoride, sodium orthovanadate, sodium pyrophosphate], Protease inhibitor cocktail (Sigma Aldrich, USA), 1.5ml Eppendorf tube, Centrifuge tubes, Protein Assay Dye Reagent Concentrate (Lot no: 5000006, Bio-Rad), Standard Antibodies (5% BSA plus DI water), Microtiter Plate, Microplate spectrophotometer (Biotek, USA), Pellet Pestle Motor (Kimble, USA), Centrifuge tubes (Cat no: 05-539-8, Fischer Scientific). All material used for Western Blot assay was courtesy of Dr. Zahoor Shah's Laboratory, University of Toledo Health Science Campus (Toledo, OH, USA).

2.2.3 Gel Electrophoresis and Transfer of Proteins

Materials used to make SDS-PAGE and protein transfer was obtained from the following source: 30% Acrylamide/bis-acrylamide (Cat no: 1610156, Bio-Rad), Glass plates (Cat no: 1653311, Bio-Rad), 5-well comb (Bio-Rad), Tetramethyl ethylenediamine (TEMED) (Lot no: 51013659, GF Healthcare), Ammonium Persulfate (APS) (Lot no: 094228, Fischer Bio-Reagent), Tris-HCL pH 8.6 (resolving gel), Tris-HCL pH 6.8 (stacking gel), Ethanol 200 proof (Lot no: 2701, Decon Labs, Inc), Polyvinylidene difluoride (PVDF) transfer membrane (Cat no: IPFL00010, Immobilon-FL), Precision Plus Protein Dual Color Standards (Cat no: 1610374, Bio-Rad), 20% SDS, Tris-base (Lot no: 75825, Affymetrix Inc, OH, USA), Glycine (Lot no: 166207, Fischer BioReagents), Methanol (Lot no: 181996 , Fischer Chemical), running buffer (Tris-base, glycine, 20%SDS), transfer buffer (Tris-base, glycine, methanol), buffer tank and lid (Bio-Rad), gel electrophoresis unit, tank transfer unit, blue cooling unit, casting stand (Bio-Rad), gel

holder cassette (Bio-Rad), 3mm thick foam sponge, filter paper, IncuBlock dry block heat incubator (Denville Scientific), BioTek microplate spectrophotometer, and a vortex mixer.

2.2.4 Western Blot Antibody Staining

Materials used for antibody staining was 5% non-fat milk [Non-fat dry milk (Lot no: 1219-2, Lab Scientific) plus 1x TBST], Tween-20 (Lot no: 110915 , Fischer Scientific), Caspase-3 Rabbit monoclonal antibody (Cat no: 9665-S, Cell Signaling Technology), Cleaved Caspase-3 Rabbit monoclonal antibody (Cat no: 9664-S, Cell Signaling Technology), Beta-actin antibody (Cat no: 4967, Cell Signaling Technology), Anti Rabbit IgG, HRP-linked Antibody (Cat no: 7074-S, Cell Signaling Technology), 1x TBST (Tris-base, NaCl and 0.1% Tween), Tris-base (Lot no: 75825, Affymetrix Inc, OH, USA) and pipettes that accurately deliver 4 µL, 10 µL, 20 µL, 1000 µL.

2.2.5 Immunodetection and Imaging

Super Signal West Pico PLUS Luminol/Enhancer Solution (Lot no: UK293299, Thermo Scientific), Super Signal West Pico PLUS Stable Peroxide solution (Lot no: UK293300, Thermo Scientific), Tweezers, Filter sponges, Small Tupperware rectangular with lid, Syngene™ GBOX-CHEMI-XX6 imager.

2.3 Whole-mount Immunofluorescence Staining Protocol

At 5-dpf, larval zebrafish were exposed to MA at three different concentrations: 0 mM (control), 5 mM, and 15 mM via immersion for five hours using a 6 well-plate as shown in Figure 6. The concentration above was used because in preliminary studies that was conducted by exposing 5-dpf larval zebrafish in 5 mM, 15 mM, 25 mM and 50 mM of MA, subjects in 25 mM and 50 mM were dead and showed signs of tissue disintegration almost an hour after exposure and within minutes in the 50 mM concentration (Wisner, Chen, unpublished results). Desired concentrations were obtained from diluting stock solution of 100 mM MA with egg water. Each concentration had two wells with five larval zebrafish (N= 5 per well) initially exhibiting normal healthy behavior (e.g. actively swimming, inflated swim bladder). 500 µL of MA was added to each well to bring the concentration to 5 mM and 15 mM respectively and 500 µL of egg water was used for the control group. Heart rate was calculated manually and using a stopwatch at every hour for 20 seconds except for the control group.

At the end of the 5-hour exposure, larval zebrafish were transferred into a glass vial to be fixed in 10% formalin. Vials are stored upright to ensure the larval zebrafish are not stuck to the walls of the vial at 4 ˚C overnight or up to two weeks. Subjects exposed to 15mM MA were removed from MA solution at 4h in two of the independent exposures as subjects were showing signs of tissue disintegration. Subjects were then permeabilized in ice cold acetone for 10 minutes at 4 ˚C. Then, subjects were transferred to Eppendorf tubes labelled with appropriate concentrations. There were 4-5 larval zebrafish in each Eppendorf tube for each concentration. Acetone was removed. 1ml of DI water was used to wash the subjects for five minutes. Then, 1ml of 1x PBS that was autoclaved at 121 ˚C

for 20 minutes was used to wash the specimens twice for five minutes each. Subjects were blocked with 500 µL of 5% BSA for 1h at RT on a gentle shaker. Following blocking, subjects were incubated in rabbit anti-activated Caspase 3 antibody (primary antibody) (1:500) at 4˚C overnight on a gentle shaker. Washing and blocking was repeated similar to as discussed previously to incubate subjects in donkey secondary antibody to the rabbit IgG (secondary antibody) (1:500). Tubes were wrapped in aluminum foil to protect the contents from light. Protocol used in this analysis was optimized according to a published protocol by (Sorrells, Toruno et al. 2013).

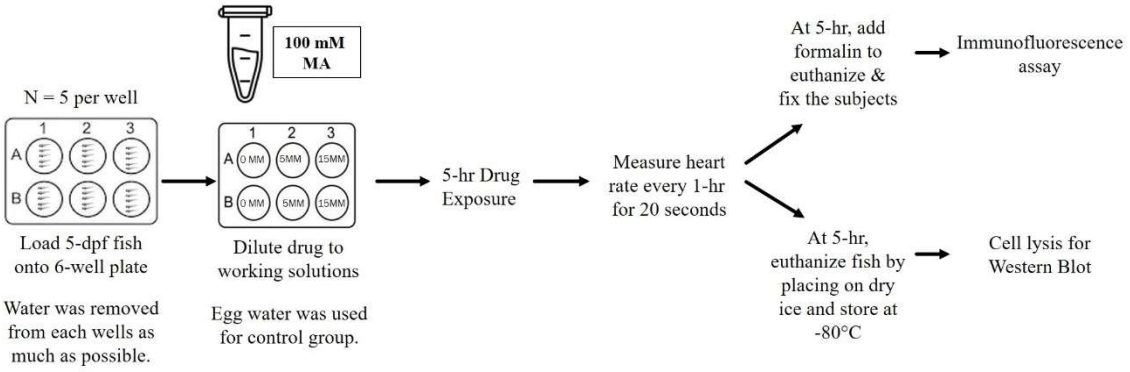

Figure 6. Schematic overview of acute MA exposure workflow in a 5-dpf larval zebrafish.

Subjects were washed with 1x PBST for five minutes. Larvae from the control group was added to a small petri dish. The petri dish was placed under a fluorescence microscope with the appropriate light filter to analyze the results. A Nikon SMZ18 stereo microscope with a blue light filter was used to analyze the fluorescent images. A snapshot of images that showed cell death for each concentration was taken for analysis. These steps were repeated for subjects exposed to 5 mM and 15 mM of MA. Larvae from each concentration were returned to their respective Eppendorf tubes and were stored at 4 ˚C.

2.4 Western Blotting Protocol

2.4.1 Drug Treatment

Five-day old larval zebrafish were exposed to MA at three different concentrations: 0mM (control), 5mM, and 15mM via immersion for five hours using a 6 well-plate as described in Figure 6. At the end of the 5-hour exposure, larval zebrafish were transferred into an Eppendorf tube labelled with their appropriate concentrations. The subjects were divided into two Eppendorf tubes per concentration to hold five subjects per tube. Excess MA solution or egg water was removed using a micropipette from the vials. Eppendorf tubes were placed in a beaker filled with dry ice to snap freeze the subjects to preserve the protein levels. Tubes were stored in a -80ºC freezer until later use.

2.4.2 Tissue Homogenization and Protein Quantification

RIPA Buffer was used to perform whole cell lysis of larval zebrafish that had been exposed to MA for 5 hours. There were six Eppendorf tubes with five subjects in each tube for the following concentrations: 0mM, 5mM, and 15mM that was stored at -80ºC freezer. 200µL of cell lysis buffer was used to homogenize the subjects in each Eppendorf tube. Tissue of the subjects were homogenized using a pellet pestle motor until tissue suspension was homogenous. Samples were centrifuged for about two minutes to eliminate air bubbles that formed during homogenization. The samples were then incubated on ice for 30 minutes and mixed using a vortex mixer every 10 minutes. Samples were then centrifuged at 14000 rpm for 10 minutes at 4ºC. The supernatant was then assayed for protein quantification using Bradford Assay (Bradford 1976). Excess tissue extracts (lysate) from each sample was stored at -80ºC freezer until required for use for Sodium Dodecyl Sulfate Polyacrylamide Gel Electrophoresis (SDS-PAGE).

2.4.3 Sodium Dodecyl Sulfate Polyacrylamide Gel Electrophoresis (SDS-PAGE)

Equal amount of proteins was diluted with Laemmli SDS-PAGE sample buffer and DI water while having samples incubated in ice to prevent protein denaturation. Then, the samples were heated at 95ºC for five minutes using an IncuBlock dry block heat incubator. Samples were then centrifuged at 13000 rpm for three minutes prior to loading the wells. 100 µg of total protein was electrophoresed on a 12% resolving SDS-gel and a 5% stacking gel was made for this assay since caspase has a relatively low molecular weight. A 5-well comb was inserted immediately making sure there was no air bubble after the stacking gel solution was added. The comb was removed gently once the gel had completely polymerized. SDS-PAGE was then assembled using the gel apparatus and the wells were rinsed with running buffer. Then, the buffer tank of the gel electrophoresis unit was filled with running buffer. The first well on each gel was loaded with 5µL of the SDS-PAGE protein standard ladder. Then, 78µL of lysate for each concentration was added to each well in the following order: 0mM, 5mM, and 15mM. The SDS-PAGE was running at 60V for 30 minutes for Phase 1 and 120V for 1h 40 minutes for Phase 2 at room temperature.

2.4.4 Transfer of Proteins

After the SDS-PAGE, the gels were gently separated from the gel plates. This step was done in a tray filled with enough ice-cold transfer buffer to have the gel plates fully immersed. Gels were transferred onto a PVDF transfer membrane that has been activated in ethanol. A gel holder cassette was placed in the tray where the cathode (black) half immersed in the transfer buffer in the tray. The transfer "sandwich" was then assembled in the following sequence: 3mm thick foam sponge, filter paper, gel, transfer membrane, filter paper, and 3mm thick foam sponge. The cassette was placed in the transfer tank that is filled with ice cold transfer buffer along with a blue cooling unit inserted in the tank, ran at 110V for 1h 10 minutes.

2.4.5 Antibody Staining and Imaging

The blots were removed from the transfer tank and washed with 1x TBST for 10 minutes thrice on a gentle rocker at room temperature. Then, the blots were blocked for 1h at RT on a gentle rocker with 5% non-fat milk. Following the blocking, blots were incubated in primary antibodies (Table 1) for 48 hours at 4 ºC on a gentle rocker.

The following steps were done on a gentle rocker at RT. The blots were washed with 1x TBST thrice for 10 minutes each time and blocked for 1h using 5% non-fat milk. Following blocking, each blot was incubated with 2 µL of the anti-rabbit IgG, HRP linked secondary antibody for two hours. Then, antigens were detected by the chemiluminescence method. The Luminol/Enhancer solution was mixed with the stable peroxidase solution in a 1:1 ratio (1ml of each). The membrane was placed in between a clear plastic sheet and placed in the transilluminator of the GBOX-Chemi-XX6 imager. Images were captured using Gene Tools Software imaging system (10-30 minutes of exposure time).

Antibody	Source	Dilution	Manufacturer	Catalog Number
β-Actin	Rabbit	1:1000	Cell Signaling	4967
Caspase-3 mAb	Rabbit	1:1000	Cell Signaling	9665-S
Cleaved Caspase-3 mAb	Rabbit	1:200	Cell Signaling	9664-S
Anti-Rabbit IgG HRP	Rabbit	1:2000	Cell Signaling	7074-S

Table 1: Antibodies used in Western Blot Assay.

2.5 Statistical Analysis

Statistical analyses were carried out using GraphPad Prism version 9 statistical software. The results were expressed as the mean ± standard error mean (SEM) and analyzed using a two-way analysis of variance (ANOVA) with repeated measures, followed by Bonferroni Test for post-hoc analysis to analyze the heart rate data following acute MA exposure. One-way ANOVA followed by Tukey *post hoc* analysis was employed to analyze results from Western Blotting. ImageJ was used to conduct densitometry and quantification analysis for Western Blotting. P values of 0.05 or less were considered significant with a 95% confidence interval (CI).

Chapter 3

Results

3.1 Changes to Heart Rate and Physical Development

Heart rate of the subjects were recorded at every hour for 20 seconds up to the 5h time point in the 5mM and 15mM. Figure 7 shows the average of heart rate (bpm) obtained from all four experiments for 5mM and 15mM treatment group. This study was repeated four times independent of each other with 10 subjects for each concentration in each experiment (n = 40). The results were qualitatively similar for each replicate. Although, heart rate was recorded at 5h, only data points until 4h was included. This is because in two of the independent exposures that was carried out, subjects were removed at 4h time point as they were showing signs of tissue disintegration and opaque appearance. Based on the graph shown in Figure 7, data shows that there was a slight decrease in heart rate for the 5 mM group which was not statistically significant. However, there was a significant decline starting at 1-hr in the 15 mM group.

Although heart rate was not recorded in the 0 mM (control) group, subjects were actively swimming, did not show any morphological changes (Figure 8A) and had a beating heart throughout the 5h exposure (data not shown). Additionally, it is important to note that subjects in the 5 mM and 15 mM cohort exhibited thigmotaxis immediately after exposure to MA (Basnet, Zizioli et al. 2019). Thigmotaxis is the avoidance of open water

(in fish) or spaces in terrestrial species, with the maintenance of body position near the edge of the container or area, and is characteristic of increased anxiety-like behavior in zebrafish.

Subjects in the 5 mM cohort showed random movement involving their pectoral fin (data not shown) and relatively stagnant change in heart rate throughout the 5h exposure. There were no recognizable morphological changes that were observed under the microscope in these subjects, as shown in Figure 8B. Also, subjects did not show any signs of death (eg: opaque appearance, lack of heartbeat) at the end of 5h exposure.

Subjects in the 15 mM cohort showed a substantial decline in heart rate starting at the 1h time point and had an irregular heartbeat. The decline in heart rate for 15 mM MA was time dependent throughout the duration of exposure. Nearly all the subjects displayed morphological changes by the end of 5h time point such as deflection in the caudal fin (tail fin) (Figure 8C), notochord bend (Figure 8E) which could indicate progression of muscle spasm from the caudal fin to the spinal cord. This has been taken as a sign of tonic seizure-like activity (Wisner, Chen, Williams and Hall, unpublished results). One of the subjects also showed blood accumulation in the sinuous venous component of the heart as shown by the red arrow at the end of the 5h exposure in Figure 8F. In two of the replicates of the drug exposure that was performed, subjects were removed from the exposure at 4h as a result of subjects exhibiting signs of tissue disintegration, opaque appearance (Figure 8D) and lack of or a weak heartbeat. Subjects were then fixed in 10% formalin or frozen using dry ice.

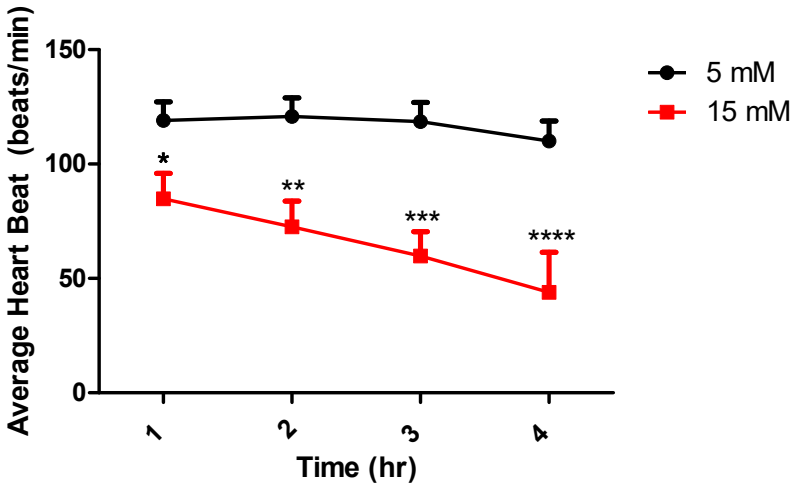

Figure 7. Outcome of acute methamphetamine exposure (5mM and 15mM) on heart rate (bpm) in 5-dpf larval zebrafish. Results shown are represented as mean ± SEM. Statistical significance determined by Bonferroni test is represented as an asterisk (*): *P ≤ 0.05, **P ≤ 0.01, ***P ≤ 0.001, ****P≤ 0.0001, ns = not significant. Some error bars are not shown because it is shorter than the size of the symbol. Four independent exposures were conducted with n = 40 for 1h to 4h for all subjects except in 15mM at 5-h, (n= 20).

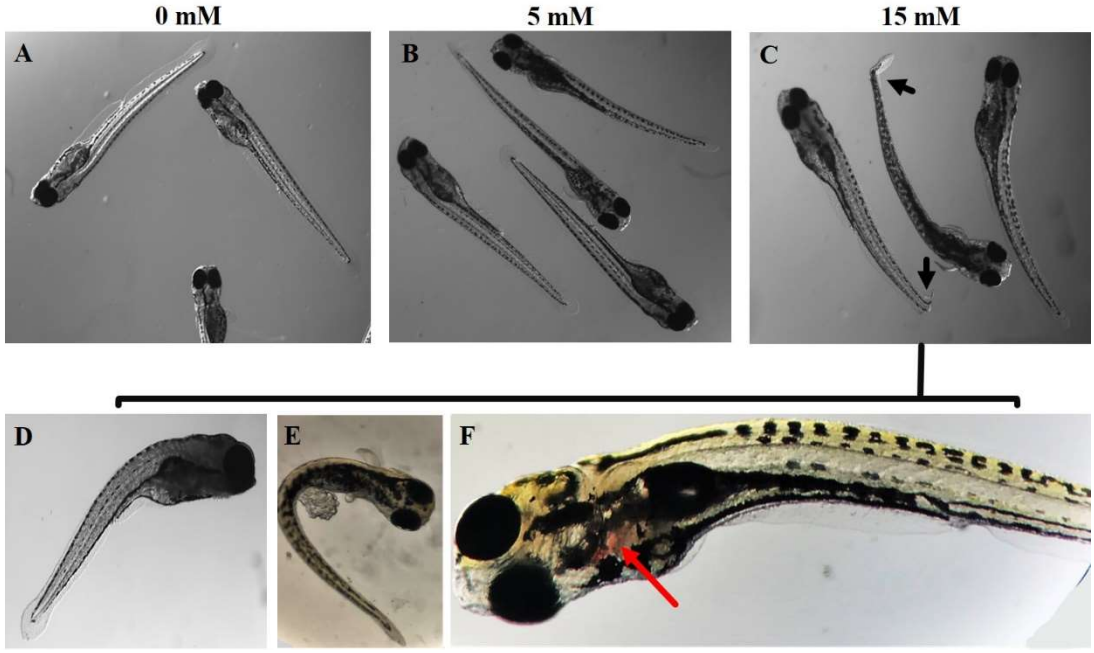

Figure 8. (A). 5-dpf larval zebrafish in the control group exposed to egg water showing no morphological changes. **(B).** 5-dpf larval zebrafish exposed to 5mM of MA for 5h showing minimal to no morphological changes. **(C).** 5-dpf larval zebrafish exposed to 15mM of MA for 5h showing morphological changes such as bent tail fin, opaque appearance **(D)**, distinct curvature of the spine **(E)** and blood accumulation in the sinuous venous component of the heart sac **(F)**

3.2 Wholemount Immunofluorescence of Caspase-3

At the end of the 5h drug exposure, the treated larvae were processed for activated (cleaved) caspase-3 immunohistochemistry. Figure 9 shows the images resulting from the Caspase-3 Immunofluorescence assay indicating presence of cleaved caspase-3.

Larvae in the control group that were exposed to egg water did show some presence of cleaved caspase-3 induced apoptosis as seen in Figure 9, however it was not as prominent as the presence of the cleaved caspase-3 in the 5mM and 15mM cohort. This may be due to normal levels of basal apoptosis associated with the subjects actively developing. Slight apoptosis can be seen around the vasculature along the notochord, closer to the caudal fin (tail fin) region as seen in the 3rd and 4th row of the 0mM column (Figure 9).

It also appears that there was elevated neuronal cell death in hindbrain and along the notochord and spinal cord in the 5mM cohort (Figure 9). A slight deflection of the caudal fin (tail fin) is seen in the 5mM column, 4th row (Figure 9). Deflection of the caudal fin was an uncommon morphological change in the 5mM cohort as compared to the subjects in the 15mM cohort.

Subjects in the 15 mM group showed a significant elevation of apoptosis compared to the 5 mM as evidenced by a more robust cluster of apoptotic cells in the hindbrain and otolith as shown in images in the 2nd row of 15mM column (Figure 9). There does not appear to be an elevation of cell death involving the heart, kidney, liver and other organs. There was also a much more notable apoptosis as bigger clusters of apoptotic cells was seen along the notochord of the larvae compared to the subjects in 5 mM. Deflection of the caudal fin (tail fin) is much more evident in the subjects exposed to 15mM of MA

which could suggest muscle contraction. Furthermore, a distinct curvature of the spinal cord was seen in images in the 2nd row of the 15mM column (Figure 9), which could be an indication of progression of muscle contraction along the entire notochord.

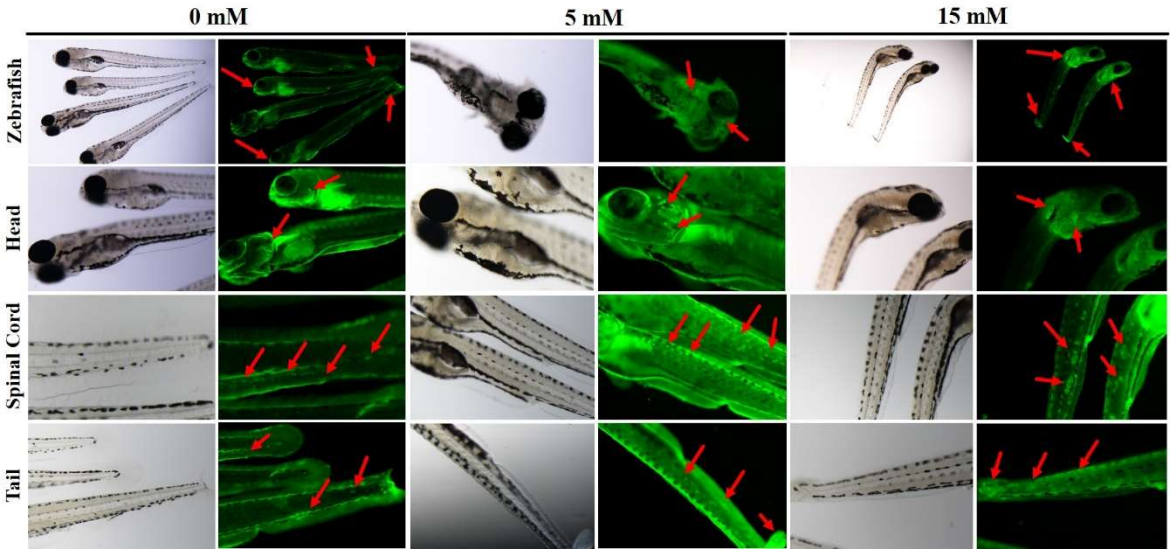

Figure 9. Represented images captured using a fluorescence microscope (Nikon SMZ18 with blue light filter) from immunostaining of caspase-3 5-dpf larval zebrafish exposed to in 0mM (control), 5mM and 15mM of MA for 5h. N= 4 to 5 per concentration.

3.3 Western Blot of Caspase-3 and Cleaved Caspase-3

Western blot analysis was used to confirm that cell death occurring in subjects exposed to MA was due to apoptosis via activation of caspase-3 to cleaved caspase-3. Western blotting was done on tissue taken from the whole larval zebrafish. As shown in Figure 10B, there was an increase in the expression of caspase-3 in the 5mM and 15mM cohort compared to the control treatment group. The difference observed was not significant [$F(2, 3) = 0.6$, NS]. Since sample size was too small, this analysis did not have enough power. The expression of cleaved caspase-3 was only visible in the 15mM cohort (Figure 10A). As for the control and 5mM treatment group, there were no visible band on the blot. Furthermore, statistical significance could not be determined for the expression of cleaved caspase-3 since there was only one blot that could be analyzed. Thus, the occurrence of apoptosis due to caspase-3 activation in the subjects acutely exposed to MA could not be confirmed, although there was a suggestion that this was occurring. However, these results can serve as preliminary data. It may be that apoptosis is not a significant part of cell death, or it could be that this data can be used to further optimize the protocol in future studies proving the presence of significant apoptosis.

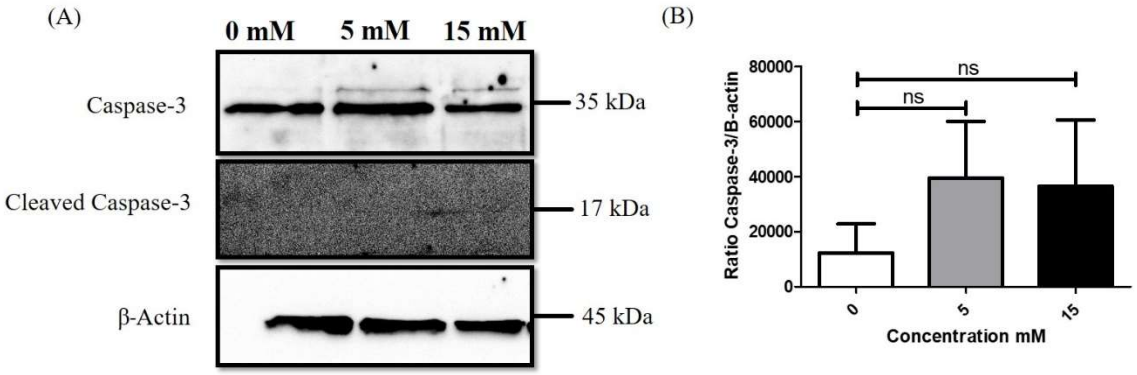

Figure 10. Two independent experiment was conducted with 10 subjects per concentration, each blot was pooled from 5 subjects. (A) Western blot analysis of caspase-3 and cleaved caspase-3 using tissue from whole larval zebrafish following acute MA exposure. (B) The protein bands were analyzed through densitometry analysis using ImageJ. The relative levels of caspase-3 expression were normalized to β-actin. Statistical significance could not be determined for the expression of cleaved caspase-3 since there was only one blot that could be analyzed. The bar graphs are presented as means ± SEM. A one-way ANOVA statistical test was employed to assess significance between 0 mM, 5mM, 15 mM of acute MA exposure followed by Tukey test to determine significance at $P < 0.05$.

Chapter 4

Conclusion

4.1 Acute Methamphetamine Exposure

The primary findings of this study show that there is evidence of slightly reduced heart rate (bradycardia) at the lower concentration of 5 mM MA compared to 15mM MA group. There was a substantial decrease in heart rate in the 15mM cohort which showed a notable decline in heart rate at around 3h after MA exposure. Subjects in the 15 mM cohort also showed prolonged periods of time between systole and diastole around the 3h time point and at the 5h time point in the 5mM cohort. It was evident that there was a poor recovery from the subjects in the 15mM cohort. Increased in myocardial contractility was also observed to be more prominent in the 5mM cohort when observed under a microscope (data not shown). However, subjects in the 15mM cohort seem to have a reduced afterload (increased resistance) in pumping blood especially after the 3h time point (data not shown). This parameter can be measured using automated video tracking tools to be able to analyze the contraction of the heart muscles in future studies. These results seem to be fairly consistent with other studies reported in humans and mice. Acute intoxication of MA typically produces initial effects such as elevated heart rate (tachycardia), hypertension, hyperthermia, increased myocardial contractility, but these effects are then followed by bradycardia, hypotension, and reduced contractility (Hassan, Wearne et al. 2016).

Although it is beyond the scope of the study to assess these parameters, hypertension and tachycardia can lead to other serious cardiovascular complications including myocardial ischemia and infarction, aortic dissection, malignant arrhythmias, stress induced cardiomyopathy and cardiac arrest (Gold and Blumenthal 2018).

4.2 Wholemount of Immunofluorescence of Caspase-3

The key goal of this assay was to determine if apoptosis is involved in neuronal or cardiomyocyte cell death. Caspase-3 is an executor caspase that can be activated via the intrinsic pathway (mitochondrial pathway) or extrinsic pathway (death-receptor pathway) as shown in Figure 5. It appears that one of mechanism that might contribute cell death in the subjects exposed to MA is apoptosis. There was some apoptosis observed in the control group where the subjects were exposed to egg water. However, that was to be expected and is most likely due to apoptosis characteristic of actively developing organisms.

Subjects exposed to 5mM MA showed some cell death due to apoptosis starting closer to the anterior head region, muscle and a very subtle manifestation of the fluorescence along the notochord and caudal fin (tail fin). Figure 11 shows a more magnified image depicting the fluorescence indicating apoptosis observed in the 5mM cohort.

Subjects exposed to 15mM of MA showed an increased level of fluorescence indicative of cell death due to apoptosis around the eye and hindbrain along with an involvement of the otolith and hindbrain as shown in the first picture in the 15mM column in Figure 11. The otolith cells project to the hindbrain and are responsible for vestibular stimuli. The nervous system in the zebrafish depends primarily on a short reflex arc to produce rapid sensory motor transformation for gaze and posture stabilization (Bagnall and Schoppik 2018). The hindbrain contains a diverse set of sensory-motor networks that control movements required for vision, respiration, mastication, and locomotion in all vertebrates (Kinkhabwala, Riley et al. 2011). Perhaps, apoptosis in the otolith and hindbrain could explain the loss of righting in these subjects following exposure to MA.

There was also a lot more notable cell death along the notochord, spinal cord of the subjects as well as the caudal fin as seen in the 2nd and 3rd image in the 15mM column (Figure 11). The bend in spinal cord (lordosis) is related to seizure like behavior in this animal model. This is one reason that can serve as evidence that neuronal cell death is involved in the overall death of subjects exposed to MA. MA is known to cause neuronal apoptosis in several brain regions, including the striatum, cortex, hippocampus and olfactory bulb (Krasnova and Cadet 2009). Neuronal cell death is believed to be due to various apoptotic pathways (Cadet, Jayanthi et al. 2005). One of the pathways involving caspase-3 discussed by Cadet, Jayanthi et al. (2005), is via activation of JNK/SAPK c-Jun pathway in rodents involving MAP kinases. MAP kinases are responsible for mediating signals from the cell membrane to the nucleus (Cadet, Jayanthi et al. 2005). Another pathway involved is via regulation of Bcl-2 family proteins (mitochondria dependent death pathway). C-jun is an activator-protein 1 (AP-1) transcription factor that contributes to MA toxicity. These are associated with an increase in caspase-3 activity as well as psychostimulant-induced poly (ADP-ribose) polymerase (PARP) cleavage in the brain due to substances (e.g. cytochrome c, apoptosis inducing factor (AIF)) released from mitochondria into the cytosol, which activates caspase-dependent executioners and promote apoptosis resulting in neurodegeneration (Cadet, Jayanthi et al. 2005, Krasnova and Cadet 2009). Moreover, MA induced cell death is found to be caused by an involvement of the Fas/FasL death pathway (extrinsic pathway) (Cadet, Jayanthi et al. 2005). FasL is a part of the tumor necrosis factor (TNF) superfamily of cytokines which is involved in multiple models of brain injury (Krasnova and Cadet 2009). Toxic doses of MA was shown to induce FasL expression in the striatum of rat. (Krasnova and Cadet

2009) also found that MA injections caused activation in pro-caspases 8 and 3, mediators of the extrinsic pathway as well as was signifying the possibility of DA playing a role in the activation of this pathway.

To our surprise, it appears that there was no pronounced apoptosis involving the heart or cardiac muscles. It is beyond the scope of this study to explain the mechanism of cardiotoxic effects, but these do not seem to involve apoptosis. Other techniques like Hematoxylin and Eosin (H&E) staining, terminal deoxynucleotidyl transferase dUTP nick end labeling (TUNEL) assay, can be used in future studies that could further analyze and possibly elucidate the mechanism involved in cardiotoxic effects induced by MA exposure. It might also involve a non-apoptotic form of cell death that does not involve caspase-3. Although, there are limited studies in zebrafish that have studied the cardiotoxic effects induced by acute MA exposure, a study in rats was shown to cause cardiac lesions in animals that were kept in warm and humid conditions (Kaiho and Ishiyama 1989). The cardiac lesions observed was characterized by necrotic myocardial lesions with myoglobin loss, widely dispersed ventricular wall and ultrastructural alteration due to prominent mitochondrial swelling, packing of cellular constituents and membrane disruption (Kaiho and Ishiyama 1989) .

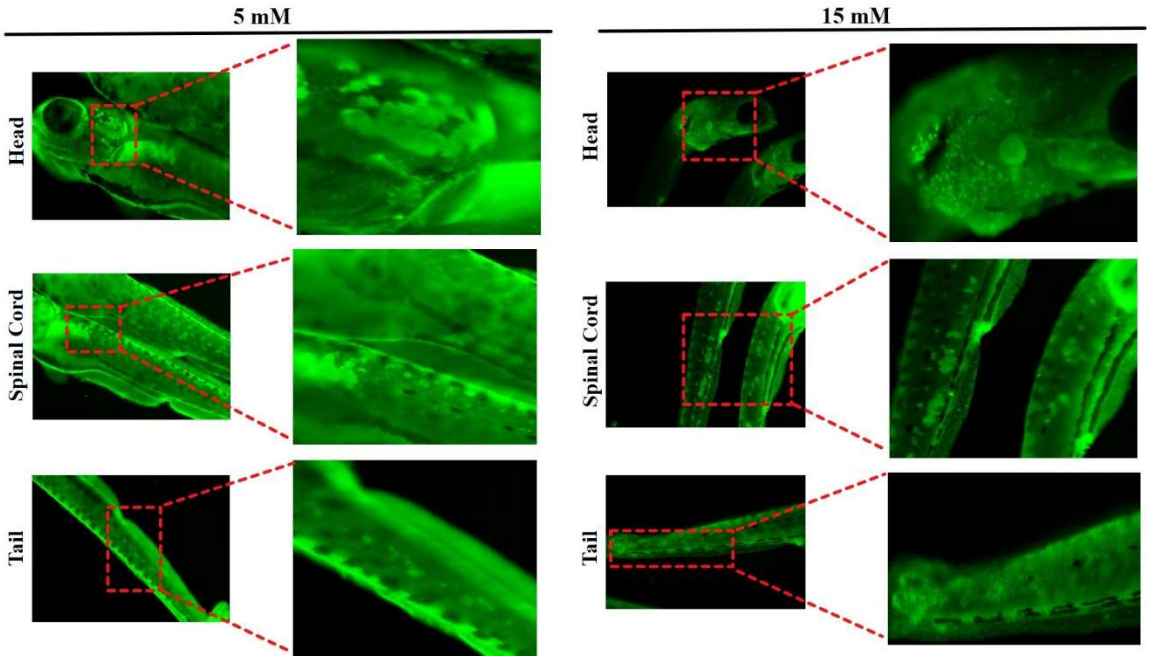

Figure 11. Enlarged images captured using a fluorescence microscope (Nikon SMZ18 with blue light filter) from immunofluorescence staining of Caspase-3 in larval zebrafish exposed to 5mM and 15mM MA, n = 4-5 per group.

4.3 Expression of Caspase-3 and Cleaved Caspase-3

Western blot was conducted to determine the presence and level of protein expression of cleaved caspase-3 to confirm that apoptosis caused cell death in the subjects that were exposed to 5mM and 15mM of MA for 5h. The protein of interest in this study is capsase-3 (35 kDa) and cleaved caspase-3 (15-17 kDa) which is the activated form of caspase-3. As shown in Figure 10, all the samples from 0mM, 15mM and 15mM showed presence of beta-actin and caspase-3. However, only samples from subjects in the 15mM cohort showed presence of the cleaved caspase-3 protein. This could perhaps be due to requiring a higher amount of total protein to be used; (100 μg was used in this study), adding the cleaved caspase-3 antibody to membranes that were stripped twice. Stripping the membrane could cause loss of antigen and protein degradation. Few other potential causes are signal from chemiluminescent substrate is too weak or antigen is masked by blocking buffer. Nevertheless, data obtain above can serve as reference to conduct additional studies hereafter utilizing a more optimized protocol.

4.4 Limitation of the Study

The zebrafish model has developed into a powerful model organism in research in translational neuroscience, behavioral studies and cardiovascular research. Nevertheless, as a novel model organism, the zebrafish has its own challenges and limitations. Due to its very small size especially in larval stage (~4mm) (Ingebretson and Masino 2013), microscope use was one of the limitations. Light microscope used in our laboratory can only magnify up to 5x. Hence, it was challenging to capture images focusing the heart of the subjects during and after the 5-hr MA exposure. In addition, their small size also made it challenging to obtain sufficient quantities of tissue samples required for protein quantification for western blotting. Secondly, the number of experiments repeated for western blot analysis was too small. An N of 4 should be done at the least in future studies. Thirdly, heart rate of the subjects in the control treatment group should be recorded to strengthen the significance of data. Lastly, since zebrafish is still a fairly new animal model, they have a limited number of zebrafish specific antibodies that can be utilized for immunohistochemistry compared to other animal models (Gut, Reischauer et al. 2017). With that said, it is important to note that every non-primate model organism has some drawbacks. The various strengths of zebrafish model as discussed above is capable of laying a promising groundwork for design of disease, drug discovery and neurobehavioral research.

4.5 Future Aspects

It is important to validate that apoptosis is involved in causing cell death secondary to acute MA exposure. Although most studies that were used to compare the results from this specific study involved other animal models, it is important to note that there is evidence of acute MA exposure causing neuronal cell death, possibly involving multiple apoptotic pathways (Hooper and Killick , Cadet, Jayanthi et al. 2005, Krasnova and Cadet 2009, M Chiu and O Schenk 2012) . Although most studies (He, Matoba et al. 1996, Craig, Gilday et al. 2006, Kaye, McKetin et al. 2007, Tomita, Okuyama et al. 2013, Courtney and Ray 2014, Hassan, Wearne et al. 2016, Darke, Duflou et al. 2017, Gold and Blumenthal 2018, Kevil, Goeders et al. 2019), that have looked into cardiovascular complications in MA-users or other animal studies involve chronic MA use, MA is believed to promote cardiovascular complications via its direct effects or catecholamine toxicity on cardiac and vascular tissue (Kevil, Goeders et al. 2019), even under conditions of acute overdose (Kaiho and Ishiyama 1989, Fang, Zhu et al. 2016). Based on the observations from our study, it is crucial to note that there was cardiovascular involvement due to MA exposure. As an evidence, MA exposure in these 5-dpf subjects caused bradycardia that became more severe over the 5h exposure to eventually very slow heartbeat or an absence of heartbeat. Cardiovascular complications are evident in MA users as seen in many other studies. To validate this finding in zebrafish, future studies can utilize techniques like TUNEL assay to detect DNA fragmentation which occurs in the last phase of apoptosis. Histochemistry using H&E staining can be done to focus primarily on the heart of the subjects exposed to different concentrations of MA to investigate if there is any damage involving the vasculature, myocardium, or heart valves and possibly elucidate a mechanism involved in

leading to cell death in the heart muscles or other cardiac impairments. Quantification of apoptotic cells observed in the immunofluorescence assay should also be carried out to provide a quantitative data. Furthermore, high speed video imaging can be employed to determine heart rate, change in the size of heart as well as observe the variance in cardiac contractility. Cardiac output can also be measured by multiplying bpm with ventricular stroke volume. To calculate stroke volume, a published protocol by (Hou and Burggren 1995) was used as reference (Chen, unpublished results). On the other hand, PARP antibody can be used in future studies as an additional apoptosis marker in Western Blotting as it is associated with activating caspase-dependent executioners and promote apoptosis resulting in neurodegeneration (Krasnova and Cadet 2009). A few techniques like lactate dehydrogenase (LDH) assay and flow cytometry or fluorescence microscopy using propidium iodide (PI) and nucleic acid stain 4′, 6′-diamidino-2-phenylindole (DAPI) to assess cell death due to necrosis (Cummings and Schnellmann 2004). Cell death due to necrosis is characterized by swelling of cell and organelle, pyknosis, increased permeability, chromatin condensation and nuclear fragmentation. LDH and PI is a conventional marker for loss of membrane integrity and presence of necrosis (Cummings and Schnellmann 2004, Chan, Moriwaki et al. 2013). Lastly, thermal regulation could be considered to see if hyperthermia is observed in the subjects exposed to MA since thermal dysregulation seem to be an important factor contributing to MA induced neurotoxicity (Krasnova and Cadet 2009).

References

Akhgari, M., H. Mobaraki and A. Etemadi-Aleagha (2017). "Histopathological study of cardiac lesions in methamphetamine poisoning-related deaths." DARU Journal of Pharmaceutical Sciences **25**(1): 5.

Anglin, M. D., C. Burke, B. Perrochet, E. Stamper and S. Dawud-Noursi (2000). "History of the methamphetamine problem." Journal of psychoactive drugs **32**(2): 137-141.

Antinucci, P. and R. Hindges (2016). "A crystal-clear zebrafish for in vivo imaging." Scientific reports **6**(1): 1-10.

AOAAM. (2019). "The Neurobiology of Addiction." Retrieved Oct 1st, 2020, from https://aoaam.org/resources/Documents/2019%20%20Spring%20Conference%20Slides/Slides%20-%20Neurobiology%20of%20addiction%20-%20Haliburda%20%20reviewed.pdf.

Asnani, A. and R. T. Peterson (2014). "The zebrafish as a tool to identify novel therapies for human cardiovascular disease." Disease Models & Mechanisms **7**(7): 763-767.

Bagnall, M. W. and D. Schoppik (2018). "Development of vestibular behaviors in zebrafish." Current opinion in neurobiology **53**: 83-89.

Bakkers, J. (2011). "Zebrafish as a model to study cardiac development and human cardiac disease." Cardiovascular research **91**(2): 279-288.

Basnet, R. M., D. Zizioli, S. Taweedet, D. Finazzi and M. Memo (2019). "Zebrafish larvae as a behavioral model in neuropharmacology." Biomedicines **7**(1): 23.

Bradford, M. M. (1976). "A rapid and sensitive method for the quantitation of microgram quantities of protein utilizing the principle of protein-dye binding." Analytical biochemistry **72**(1-2): 248-254.

Burke, E. (August 9, 2016). "Why Use Zebrafish to Study Human Diseases?" I am Intramural Blog Retrieved September 22, 2020, from https://irp.nih.gov/blog/post/2016/08/why-use-zebrafish-to-study-human-diseases.

Cadet, J. L., S. Jayanthi and X. Deng (2005). "Methamphetamine-induced neuronal apoptosis involves the activation of multiple death pathways. Review." Neurotoxicity research **8**(3-4): 199-206.

Chan, F. K.-M., K. Moriwaki and M. J. De Rosa (2013). Detection of necrosis by release of lactate dehydrogenase activity. Immune Homeostasis, Springer**:** 65-70.

Courtney, K. E. and L. A. Ray (2014). "Methamphetamine: an update on epidemiology, pharmacology, clinical phenomenology, and treatment literature." Drug and alcohol dependence **143**: 11-21.

Craig, M. P., S. D. Gilday and J. R. Hove (2006). "Dose-dependent effects of chemical immobilization on the heart rate of embryonic zebrafish." Lab Anim (NY) **35**(9): 41-47.

Cruickshank, C. C. and K. R. Dyer (2009). "A review of the clinical pharmacology of methamphetamine." Addiction **104**(7): 1085-1099.

Cummings, B. S. and R. G. Schnellmann (2004). "Measurement of cell death in mammalian cells." Current protocols in pharmacology **25**(1): 12.18. 11-12.18. 22.

d'Amora, M. and S. Giordani (2018). "The Utility of Zebrafish as a Model for Screening Developmental Neurotoxicity." Frontiers in Neuroscience **12**(976).

Darke, S., J. Duflou and S. Kaye (2017). "Prevalence and nature of cardiovascular disease in methamphetamine-related death: a national study." Drug and alcohol dependence **179**: 174-179.

Drugs, U. N. O. o. and Crime (2020). World Drug Report 2020: Drug Use and Health Consequences. World Drug Report, United Nations Office on Drugs and Crime.

Elmore, S. (2007). "Apoptosis: a review of programmed cell death." Toxicologic pathology **35**(4): 495-516.

Fang, J., D. Zhu and C. Luo (2016). "An In Vivo Assessment: Cardiotoxicity Induced by Three Kinds of Addictive Drugs (Methamphetamine, Ketamine, and Methadone) in Zebrafish Embryos." International Journal of Public Health and Safety **1**(3).

Ferrucci, M., F. Limanaqi, L. Ryskalin, F. Biagioni, C. L. Busceti and F. Fornai (2019). "The effects of amphetamine and methamphetamine on the release of norepinephrine, dopamine and acetylcholine from the brainstem reticular formation." Frontiers in neuroanatomy **13**: 48.

Galanternik, M. V., A. N. Stratman and B. M. Weinstein (2020). The Zebrafish Cardiovascular System. The Zebrafish in Biomedical Research, Elsevier**:** 131-143.

Gold, M. and D. M. Blumenthal. (2018). "Q&A: Daniel M. Blumenthal, MD, MBA Substance Abuse And Cardiovascular Disease." Retrieved 11/15/2020, 2020, from https://www.rivermendhealth.com/resources/qa-daniel-blumenthal-abuse-cardiovascular-disease.

Gut, P., S. Reischauer, D. Y. Stainier and R. Arnaout (2017). "Little fish, big data: zebrafish as a model for cardiovascular and metabolic disease." Physiological reviews **97**(3): 889-938.

Gutierrez-Lovera, C., A. Vazquez-Rios, J. Guerra-Varela, L. Sanchez and M. De la Fuente (2017). "The potential of zebrafish as a model organism for improving the translation of genetic anticancer nanomedicines." Genes **8**(12): 349.

Haile, C. N. (2008). "Neurochemical and neurobehavioral consequences of methamphetamine abuse." Neurochemistry.

Hassan, S. F., T. A. Wearne, J. L. Cornish and A. K. Goodchild (2016). "Effects of acute and chronic systemic methamphetamine on respiratory, cardiovascular and metabolic function, and cardiorespiratory reflexes." The Journal of Physiology **594**(3): 763-780.

Haupt, S., M. Berger, Z. Goldberg and Y. Haupt (2003). "Apoptosis - the p53 network." Journal of Cell Science **116**(20): 4077-4085.

He, S.-Y., R. Matoba, N. Fujitani, K.-i. Sodesaki and S. Onishi (1996). "Cardiac muscle lesions associated with chronic administration of methamphetamine in rats." The American journal of forensic medicine and pathology **17**(2): 155-162.

Hedegaard, H., A. M. Miniño and M. Warner (2020). Drug Overdose Deaths in the United States, 1999–2018. S. National Center for Health. Hyattsville, MD, National Center for Health Statistics. **356**.

Hooper, C. and R. Killick. "Neuronal degeneration through inappropriate activation of apoptotic cell-death pathways explained. Mechanisms and key protein players." Retrieved 10/25/20, 2020, from https://www.abcam.com/content/apoptosis-mitochondrial-and-death-receptor-pathways.

Hou, P. and W. W. Burggren (1995). "Cardiac output and peripheral resistance during larval development in the anuran amphibian Xenopus laevis." American Journal of Physiology-Regulatory, Integrative and Comparative Physiology **269**(5): R1126-R1132.

Ickes, J. R. (2015). The Effects of Acute and Chronic Methamphetamine Exposure on Cardiovascular Development, Developmental Rate, and Aggression in Danio rerio, University of Akron.

Ingebretson, J. J. and M. A. Masino (2013). "Quantification of locomotor activity in larval zebrafish: considerations for the design of high-throughput behavioral studies." Frontiers in neural circuits **7**: 109.

Jeong, J.-Y., H.-B. Kwon, J.-C. Ahn, D. Kang, S.-H. Kwon, J. A. Park and K.-W. Kim (2008). "Functional and developmental analysis of the blood–brain barrier in zebrafish." Brain research bulletin **75**(5): 619-628.

Kaiho, M. and I. Ishiyama (1989). "Morphological study of acute myocardial lesions experimentally induced by methamphetamine." Nihon hoigaku zasshi= The Japanese journal of legal medicine **43**(6): 460-468.

Kalueff, A. V., M. Gebhardt, A. M. Stewart, J. M. Cachat, M. Brimmer, J. S. Chawla, C. Craddock, E. J. Kyzar, A. Roth and S. Landsman (2013). "Towards a comprehensive catalog of zebrafish behavior 1.0 and beyond." Zebrafish **10**(1): 70-86.

Kaye, S., R. McKetin, J. Duflou and S. Darke (2007). "Methamphetamine and cardiovascular pathology: a review of the evidence." Addiction **102**(8): 1204-1211.

Kevil, C. G., N. E. Goeders, M. D. Woolard, M. S. Bhuiyan, P. Dominic, G. K. Kolluru, C. L. Arnold, J. G. Traylor and A. W. Orr (2019). "Methamphetamine Use and Cardiovascular Disease: In Search of Answers." Arteriosclerosis, thrombosis, and vascular biology **39**(9): 1739-1746.

Khan, K. M., A. D. Collier, D. A. Meshalkina, E. V. Kysil, S. L. Khatsko, T. Kolesnikova, Y. Y. Morzherin, J. E. Warnick, A. V. Kalueff and D. J. Echevarria (2017). "Zebrafish models in neuropsychopharmacology and CNS drug discovery." British Journal of Pharmacology **174**(13): 1925-1944.

Kinkhabwala, A., M. Riley, M. Koyama, J. Monen, C. Satou, Y. Kimura, S.-i. Higashijima and J. Fetcho (2011). "A structural and functional ground plan for neurons in the hindbrain of zebrafish." Proceedings of the National Academy of Sciences **108**(3): 1164-1169.

Kish, S. J. (2008). "Pharmacologic mechanisms of crystal meth." Cmaj **178**(13): 1679-1682.

Koob, G. F. (1992). "Drugs of abuse: anatomy, pharmacology and function of reward pathways." Trends in pharmacological sciences **13**: 177-184.

Krasnova, I. N. and J. L. Cadet (2009). "Methamphetamine toxicity and messengers of death." Brain research reviews **60**(2): 379-407.

Lawrence, C. (2007). "The husbandry of zebrafish (Danio rerio): a review." Aquaculture **269**(1-4): 1-20.

Lawrence, C. (2011). The Reproductive Biology and Spawning of Zebrafish in Laboratory

Settings. Zebrafish: Methods for Assessing Drug Safety and Toxicity. P. McGrath, John Wiley & Sons**:** 1-13.

Leung, K. P., Y. H. Qu, D. F. Qiao, W. B. Xie, D. R. Li, J. T. Xu, H. J. Wang and X. Yue (2014). "Critical role of insulin-like growth factor binding protein-5 in methamphetamine-induced apoptosis in cardiomyocytes." Molecular medicine reports **10**(5): 2306-2312.

M Chiu, V. and J. O Schenk (2012). "Mechanism of action of methamphetamine within the catecholamine and serotonin areas of the central nervous system." Current drug abuse reviews **5**(3): 227-242.

Mao, L., W. Jia, L. Zhang, Y. Zhang, L. Zhu, M. U. Sial and H. Jiang (2020). "Embryonic development and oxidative stress effects in the larvae and adult fish livers of zebrafish (Danio rerio) exposed to the strobilurin fungicides, kresoxim-methyl and pyraclostrobin." Science of The Total Environment: 139031.

McCluskey, B. M. and J. H. Postlethwait (2015). "Phylogeny of zebrafish, a “model species,” within Danio, a “model genus”." Molecular Biology and Evolution **32**(3): 635-652.

Merritt, D. P. (2019). "Lecture 11 The Neurobiology of Addiction The Reward Pathway." Retrieved Oct 3rd, 2020, from https://www.youtube.com/watch?v=x0uqQYhw6Es&app=desktop.

Moorjani, N., M. Ahmad, P. Catarino, R. Brittin, D. Trabzuni, F. Al-Mohanna, N. Narula, J. Narula and S. Westaby (2006). "Activation of apoptotic caspase cascade during the transition to pressure overload-induced heart failure." Journal of the American College of Cardiology **48**(7): 1451-1458.

Mueller, T., Z. Dong, M. A. Berberoglu and S. Guo (2011). "The dorsal pallium in zebrafish, Danio rerio (Cyprinidae, Teleostei)." Brain research **1381**: 95-105.

NIDA. (2016). "The Reward Circuit: How the Brain Responds to Methamphetamine." Retrieved Sept 28th, 2020, from https://www.drugabuse.gov/videos/reward-circuit-how-brain-responds-to-methamphetamine.

NIDA. (2019). "Methamphetamine DrugFacts." Retrieved September, 29th, 2020, from https://www.drugabuse.gov/publications/drugfacts/methamphetamine.

Panula, P., Y.-C. Chen, M. Priyadarshini, H. Kudo, S. Semenova, M. Sundvik and V. Sallinen (2010). "The comparative neuroanatomy and neurochemistry of zebrafish CNS systems of relevance to human neuropsychiatric diseases." Neurobiology of disease **40**(1): 46-57.

Paratz, E. D., N. J. Cunningham and A. I. MacIsaac (2016). "The cardiac complications of methamphetamines." Heart, Lung and Circulation **25**(4): 325-332.

Poon, K. L. and T. Brand (2013). "The zebrafish model system in cardiovascular research: A tiny fish with mighty prospects." Global Cardiology Science and Practice **2013**(1): 4.

Portavella, M., B. Torres and C. Salas (2004). "Avoidance response in goldfish: emotional and temporal involvement of medial and lateral telencephalic pallium." Journal of Neuroscience **24**(9): 2335-2342.

Reddy, P. K., T. M. Ng, E. E. Oh, G. Moady and U. Elkayam (2020). "Clinical Characteristics and Management of Methamphetamine-Associated Cardiomyopathy: State-of-the-Art Review." Journal of the American Heart Association **9**: e016704.

Reed, B. and M. Jennings (2011). "Guidance on the housing and care of zebrafish danio rerio." Guidance on the housing and care of zebrafish Danio rerio.

Rink, E. and M. F. Wullimann (2002). "Development of the catecholaminergic system in the early zebrafish brain: an immunohistochemical study." Developmental brain research **137**(1): 89-100.

Rothman, R. B., M. H. Baumann, C. M. Dersch, D. V. Romero, K. C. Rice, F. I. Carroll and J. S. Partilla (2001). "Amphetamine-type central nervous system stimulants release norepinephrine more potently than they release dopamine and serotonin." Synapse **39**(1): 32-41.

Rubinstein, A. L. (2006). "Zebrafish assays for drug toxicity screening." Expert opinion on drug metabolism & toxicology **2**(2): 231-240.

Sallinen, V., M. Sundvik, I. Reenilä, N. Peitsaro, D. Khrustalyov, O. Anichtchik, G. Toleikyte, J. Kaslin and P. Panula (2009). "Hyperserotonergic phenotype after monoamine oxidase inhibition in larval zebrafish." Journal of neurochemistry **109**(2): 403-415.

Sofuoglu, M. and R. A. Sewell (2009). "Norepinephrine and stimulant addiction." Addiction biology **14**(2): 119-129.

Sorrells, S., C. Toruno, R. A. Stewart and C. Jette (2013). "Analysis of Apoptosis in Zebrafish Embryos by Whole-mount Immunofluorescence to Detect Activated Caspase 3." JoVE(82): e51060.

Stainier, D. Y. R. (2001). "Zebrafish genetics and vertebrate heart formation." Nature Reviews Genetics **2**(1): 39-48.

Sun, X., Y. Wang, B. Xia, Z. Li, J. Dai, P. Qiu, A. Ma, Z. Lin, J. Huang and J. Wang

(2019). "Methamphetamine produces cardiac damage and apoptosis by decreasing melusin." Toxicology and applied pharmacology **378**: 114543.

Tackie-Yarboi, E., A. Wisner, A. Horton, T. Q. Chau, J. Reigle, A. J. Funk, R. E. McCullumsmith, F. S. Hall, F. E. Williams and I. T. Schiefer (2020). "Combining Neurobehavioral Analysis and In Vivo Photoaffinity Labeling to Understand Protein Targets of Methamphetamine in Casper Zebrafish." ACS Chemical Neuroscience **11**(17): 2761-2773.

Tomita, M., T. Okuyama, H. Katsuyama, Y. Watanabe, K. Shinone, M. Nata and T. Ishikawa (2013). "Cardiotoxicity of methamphetamine under stress conditions: Comparison of single dose and long-term use." Molecular medicine reports **7**(6): 1786-1790.

Vaz, R., W. Hofmeister and A. Lindstrand (2019). "Zebrafish models of neurodevelopmental disorders: limitations and benefits of current tools and techniques." International journal of molecular sciences **20**(6): 1296.

von Trotha, J. W., P. Vernier and L. Bally-Cuif (2014). "Emotions and motivated behavior converge on an amygdala-like structure in the zebrafish." European Journal of Neuroscience **40**(9): 3302-3315.

Yifan Xiao, M., Justin Ling, MD, MS, Gil McIntire, Victoria Recalde. "Pharmacology: Psychomotor Stimulants." Retrieved Oct 2nd, 2020, from https://www.osmosis.org/learn/Psychomotor_stimulants.